SCIENTIFIC
REPORTS
natureresearch

OPEN

The diagnostic nomogram of platelet-based score models for hepatic alveolar echinococcosis and atypical liver cancer

Qiancheng Du[1,6], Yanyan Wang[2,6], Shihao Guan[3,6], Chenliang Hu[4,6], Mengxuan Li[4], Ling Zhou[1], Mengzhao Zhang[5], Yichong Chen[5], Xuepeng Mei[5], Jian Sun [1,7*] & Ying Zhou [4,7*]

Hepatic alveolar echinococcosis (HAE) and liver cancer has similarities in imaging results, clinical characteristics, and so on. And it is difficult for clinicians to distinguish them before operation. The aim of our study was to build a differential diagnosis nomogram based on platelet (PLT) score model and use internal validation to check the model. The predicting model was constructed by the retrospective database that included in 153 patients with HAE (66 cases) or liver cancer (87 cases), and all cases was confirmed by clinicopathology and collected from November 2011 to December 2018. Lasso regression analysis model was used to construct data dimensionality reduction, elements selection, and building prediction model based on the 9 PLT-based scores. A multi-factor regression analysis was performed to construct a simplified prediction model, and we added the selected PLT-based scores and relevant clinicopathologic features into the nomogram. Identification capability, calibration, and clinical serviceability of the simplified model were evaluated by the Harrell's concordance index (C-index), calibration plot, receiver operating characteristic curve (ROC), and decision curve. An internal validation was also evaluated by the bootstrap resampling. The simplified model, including in 4 selected factors, was significantly associated with differential diagnosis of HAE and liver cancer. Predictors of the simplified diagnosis nomogram consisted of the API index, the FIB-4 index, fibro-quotient (FibroQ), and fibrosis index constructed by King's College Hospital (King's score). The model presented a perfect identification capability, with a high C-index of 0.929 (0.919 through internal validation), and good calibration. The area under the curve (AUC) values of this simplified prediction nomogram was 0.929, and the result of ROC indicated that this nomogram had a good predictive value. Decision curve analysis showed that our differential diagnosis nomogram had clinically identification capability. In conclusion, the differential diagnosis nomogram could be feasibly performed to verify the preoperative individualized diagnosis of HAE and liver cancer.

Hepatic alveolar echinococcosis (HAE), also known as hepatic malignant parasitic disease, is an ancient zoonotic parasitic disease[1]. In recent years, HAE has become a worldwide epidemic disease that seriously endangers the world's public health and economic development with the development of tourism, the flow of population and the rapid increase of domestic dogs[2]. HAE proliferates by the means of budding or infiltration, which could produce new vesicles that infiltrated into the deep tissue. HAE could not only directly infiltrate the adjacent tissue, but also could be moved to the peritoneum and distant organs through lymphatic channels and blood vessels[3]. The diagnosis of HAE mainly depends on epidemiological evidence, clinical characteristics, serology and immunological

[1]Department of General Surgery, Shanghai Fourth People's Hospital Affiliated to Tongji University School of Medicine, Shanghai, 200081, China. [2]Department of Hematology, Fuyang Hospital of Anhui Medical University, Fuyang, 236000, China. [3]Department of Plastic surgery, the Qingpu Branch of Zhongshan Hospital Affiliated to Fudan University, Shanghai, 201700, China. [4]Department of Hepatopancreatobiliary Surgery, the Affiliated Hospital of Qinghai University and Qinghai Province Key Laboratory of Hydatid Disease Research, Qinghai University, Xining, 81000, China. [5]The Graduate School, Qinghai University, Xining, 810000, China. [6]These authors contributed equally: Qiancheng Du, Yanyan Wang, Shihao Guan and Chenliang Hu. [7]These authors jointly supervised this work: Jian Sun and Ying Zhou. *email: 13311856338@163.com; 17697227511@163.com

test, imaging examination, and other factors[4]. Clinical features of HAE are atypical, and the imaging features of HAE are similar to those of liver cancer, such as space-occupying lesion and irregular liquid dark areas. In addition, the enhanced CT scanning could also display the result of local enhancement for calcified HAE lesions. Therefore, an experienced surgeons sometimes has difficulty in distinguishing HAE from atypical liver cancer, especially in liver cancer with low alpha-fetoprotein (AFP) levels.

Radical hepatectomy is the first choice for the treatment of HAE and liver cancer[5,6]. For patients with liver cancer, if they exist extrahepatic metastasis, then they have lost the opportunity of radical surgery[7]. However, extrahepatic metastasis such as lungs, brain is not an absolute contraindication to HAE[8]. For brain metastasis, patients could still be treated with surgery combined with medication [albendazole, 0–15 mg/(kg●d)] as long as lesions do not metastasize to the functional areas of the brain. Similarly, hepatectomy combined with pulmonary lobectomy could also be performed for the treatment of patients with pulmonary metastasis[9,10]. It is important to accurately diagnose HAE and liver cancer before surgery because different diseases are treated in a completely different way. Therefore, given the significance of diagnosing definitely these two diseases, it is necessary to construct simple diagnostic models without performing liver biopsy before surgery.

Chronic hepatitis, posthepatitic cirrhosis and liver cancer are the three phases of disease development. However, patients with HAE, including hepatitis and non-hepatitis, have no clinically significant liver fibrosis in clinical practice. Thus, we wonder if HAE and atypical liver cancer could be distinguished that based on the prediction model of liver fibrosis. A noninvasive prediction model based on platelet (PLT) have already been widely applied, and could be an effective approach to evaluate the extent of liver fibrosis. The King's Score (fibrosis index constructed by King's College Hospital), the FibroQ (Fibro-quotient), and other score models have been reported that they could accurately predict liver fibrosis, liver cirrhosis and liver functional damage in patients with chronic hepatitis[11–13]. However, the noninvasive prediction models based on PLT for probability of diagnosing HAE and atypical liver cancer are still rare, especial in selecting optimum diagnostic models.

Currently, nomograms have been developed in the tumor diseases and non-tumor diseases, however, it is rarely used in the differential diagnosis of tumor diseases and non-tumor diseases. In our study, we point out a feasible simplified nomogram based on PLT models that selected by the least absolute shrinkage and selection operator (LASSO) regression analysis and verify it with bootstrapping validation.

Results

Patient characteristics. The baseline data of 153 patients are listed in Table 1. The median age of 153 patients is 49.1 (range 24–76) years. Ninety nine (64.7%) patients are males and 54 (35.3%) patients are females. All patients are positive for hepatitis B surface antigen (HBsAg), HBe antigen (HBeAg) or anti-HBe antibody (HBeAb), hepatitis B core antibody (HBcAb). The univariate analysis shows that the PLT ($P < 0.001$), API (age/platelet count index) ($P < 0.001$), CDS (cirrhosis discriminant score) ($P < 0.001$), FIB-4 (fibrosis index based on the four factors) ($P < 0.001$), FibroQ ($P < 0.001$), GUCI (Goteburg University Cirrhosis Index) ($P < 0.001$), King's score ($P < 0.001$), Pohl score ($P < 0.001$), and AARP (AAR, Aspartate aminotransferase/alanine aminotransferase ratio; AARP, AAR-platelet count score) ($P < 0.001$) have obvious difference between HAE group and liver cancer group.

Diagnostic potential of the PLT-based score models. The ROC is performed to evaluate the potential of PLT-based score models as biomarkers for HAE and liver cancer (Fig. 1). The AUC of PLT is 0.854 [95% confidence interval (CI), 0.785–0.906; $P < 0.001$] and the optimum cutoff value of this score model is 200. The AUC of API is 0.898 (95% CI, 0.839–0.941; $P < 0.001$) and the optimum cutoff value of this score model is 5. The AUC of CDS is 0.825 [95% CI, 0.755–0.882; $P < 0.001$), 0.788–0.906; $P < 0.001$] and the optimum cutoff value of this score model is 5. The AUC of FIB-4 is 0.931 (95% CI, 0.879–0.966; $P < 0.001$) and the optimum cutoff value of this score model is 1.64. The AUC of FibroQ is 0.882 (95% CI, 0.820–0.929; $P < 0.001$) and the optimum cutoff value of this score model is 3.11. The AUC of GUCI is 0.701 (95% CI, 0.621–0.772; $P < 0.001$) and the optimum cutoff value of this score model is 43.38. The AUC of King's score is 0.920 (95% CI, 0.866–0.958; $P < 0.001$) and the optimum cutoff value of this score model is 9.41.

Factors selection. Of PLT-based score models, 9 factors are reduced to four possible indicators based on 153 patients in the primary cohort (2:1 ratio; Fig. 2A,B), and these factors characterized by nonzero coefficients in the LASSO regression analysis model. These factors included API, FIB-4, FibroQ, and King's score. API is a model based on age and platelet count. When this score reached 5, liver biopsy could be avoided because of its high predictive value between HAE and liver cancer. FIB-4 could prove worthy as a simple model to predict probability of malignant tumor. Our study presents that FIB-4 more than 1.64 have a high risk of live cancer. FibroQ, named fibro-quotient, is also a noninvasive model have been proposed to estimate the severity of hepatic fibrosis. Our result shows that FibroQ >3.11 could significantly distinguish HAE or liver cancer. King's score, constructed by King's College Hospital, is a feasible index for predicting cirrhosis. King's score more than 9.41 have a high risk of liver cancer.

Constructing a simplified prediction model. Results of binomial logistic regression analysis model for API, FIB-4, FibroQ, and King's score that selected by the LASSO regression model are given in Fig. 3. The results shows that King's score is an independent risk factor for distinguishing HAE from liver cancer (95% CI, 1.040–30.575; $P = 0.0388$). However, the AUC of ROC curve after combining King's score, API, FIB-4, and FibroQ is 0.932, which is significantly higher than that of each independent factor (Fig. 1H). This indicates that the independent risk factor combined with the other three factors has more diagnostic value. The model that incorporates the above possible predictive factors is constructed and showed as the visualization nomogram (Fig. 4).

Variables	HAE group n = 66	Liver cancer group n = 87	All Patients n = 153
Demographics			
Age (Year)	43.00 (30.75–50.75)	54.00 (48.00–63.00)	50.00 (44.00–60.00)
Sex			
male	28 (28.3%)	71 (71.7%)	99
female	38 (70.4%)	16 (29.6%)	54
Maximum diameter of lesion	11.46 (7.12–14.37)	7.00 (4.00–10.00)	8.00 (5.00–12.00)
Extrahepatic metastasis			
No	49 (41.5%)	69 (58.5%)	118
Yes	17 (48.6%)	18 (51.4%)	35
Therapy method			
Radical surgery	31 (46.3%)	36 (53.7%)	67
Non-surgical treatment	35 (40.7%)	51 (59.3%)	86
Child-Pugh classification			
A	41 (35.3%)	75 (64.7%)	116
B	23 (65.7%)	12 (34.3%)	35
C	2 (100%)	0 (0%)	
Biochemical markers			
Hemoglobin	126.91 ± 29.38	148.74 ± 21.95	139.32 ± ?.56
ALT	28.50 (19.00–49.00)	43.00 (30.00–71.00)	?3.61 (25.00–58.50)
AST	28.00 (22.00–42.00)	52.00 (38.00–?)	?.21 (28.00–60.00)
PLT	238.00 (182.75–312.00)	128.00 (8?.00–15?.00)	183.80 (113.50–239.50)
INR	1.07 (0.96–1.26)	1.10 (0.98–1.?)	1.11 (0.98–1.24)
PT	12.80 (11.48–15.25)	1?.00 (11.80–14.?)	12.90 (11.70–14.95)
APTT	35.90 (31.43–40.35)	33.?0 (?–37.20)	34.70 (30.50–38.80)
PLT-based models			
API	2.00 (1.00–5.00)	7.00 (?.00–8.00)	6.00 (2.00–8.00)
CDS	4.00 (3.00–6.0?)	6.00 (6.00–7.00)	6.00 (4.00–7.00)
FIB-4	0.89 (0.63–1.3?)	3.18 (2.49–5.56)	2.13 (0.95–3.72)
FibroQ	1.80 (1.27–2.64)	5.51 (3.65–9.82)	3.52 (1.79–6.78)
GUCI	26.?? (?.?2–42.?2)	48.96 (27.75–78.86)	39.00 (24.61–62.71)
King's score	5.38 (3.??–?.05)	26.79 (15.68–42.58)	13.38 (5.67–29.16)
Pohl score (0/1)	62/4	50/37	112/41
AARP (0/1)	??/39	9/78	36/117

Table 1. Baseline Characteristics of HAE and liver cancer. **Abbreviation**: HAE, hepatic alveolar echinococcosis; INR, international normalized ratio; PT, Prothrombin time; ALT, Alanineaminotransferase; AST, Aspartateaminotransferase; PLT, Platelet count; API, Age/ platelet count index; CDS, Cirrhosis discriminant score; FIB-4, Fibrosis index based on the four factors; FibroQ, Fibro-quotient; GUCI, Goteburg University Cirrhosis Index; King's score, Fibrosis index based on the four factors; AAR, Aspartate aminotransferase/alanine aminotransferase ratio; AARP, AAR-platelet count score.

Identification capability of differential diagnosis nomogram. The calibration curve of the prediction nomogram for the differential diagnosis of HAE and liver cancer presents a good agreement in our research (Fig. 5A). The Harrell's concordance index (C-index) for our prediction nomogram is 0.929 (0.886–0.972) for our cohort. The C-index of our nomogram is validated to be 0.919 through bootstrapping validation, and the result also demonstrated a good identification capability. The ROC curve of the differential diagnosis nomogram in the cohort is showed in Fig. 5B. The AUC values of this prediction nomogram is 0.929. The result of ROC indicates that this nomogram have a good predictive value.

The decision curve for the differential diagnosis nomogram is showed in Fig. 5C. The decision curve shows that if the threshold probability of a patient or doctor is >6%, using the nomogram to diagnose HAE or liver cancer could acquire much more benefit. And it is obvious for net benefit of the differential diagnosis nomogram within this range of threshold probability.

Discussion

It was difficult to distinguish HAE from liver cancer because HAE had no specific clinical features, and imaging examination also lacked characteristic finding. The imaging findings of HAE and liver cancer are similar, such as a large space-occupying lesion in the liver, irregular areas of reduced density, etc[14–16]. Sometimes, liver cancer is difficult to distinguish from HAE in imaging, especially for those patients with low levels of AFP. Atypical liver cancer presents cystic lesion, no pseudocapsule, no dynamic scanning enhancement, and no portal vein invasion or tumor thrombus formation in imaging finds. The gold standard that diagnosed liver lesions is histopathological
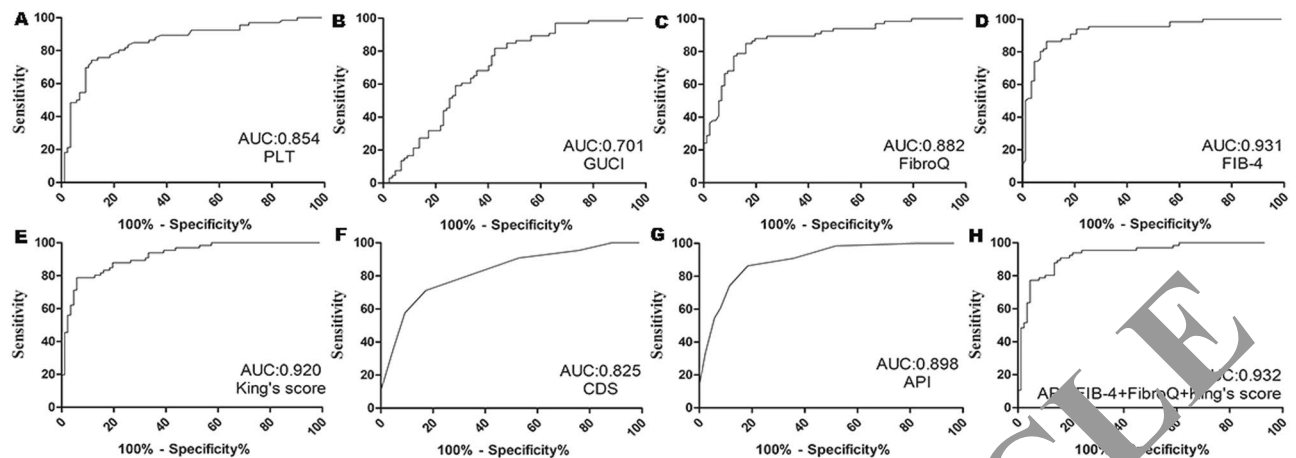
Figure 1. Receiver operating characteristic analysis using PLT, GUCI, FibroQ, FIB-4, King's score, CDS, API, and their combination in HAE group (n = 66) and liver cancer group (n = ...)
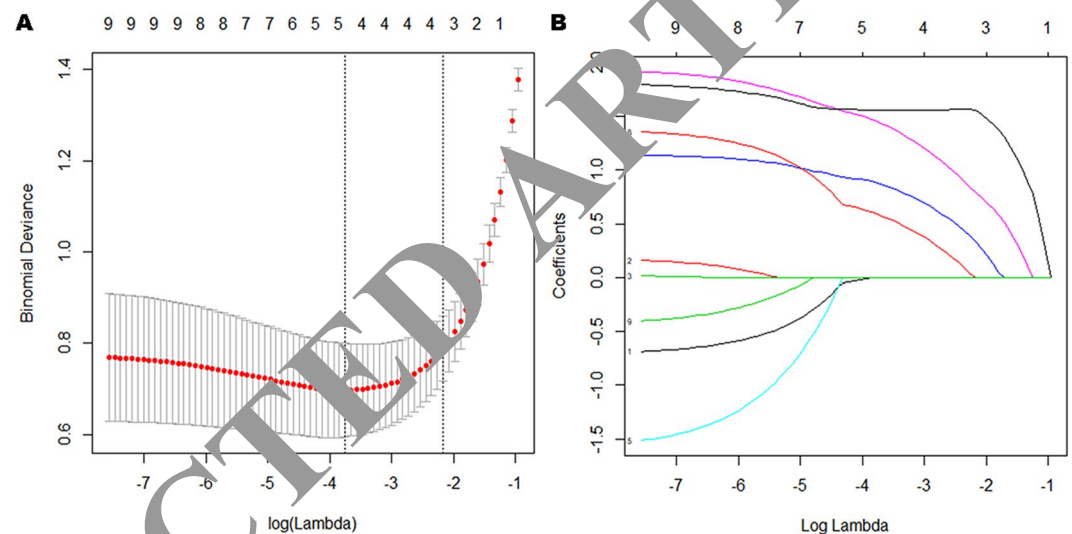

Figure 2. PLT-based score models selection using the LASSO binary logistic regression model. (**A**) The Optimum parameter (lambda) selection in the LASSO model performed fivefold cross-validation through minimum criteria. The partial likelihood deviance (binomial deviance) curve was presented versus log (lambda). Dotted vertical lines were showed at the optimum values by performing the minimum criteria and the 1-SE of the minimum criteria (the 1-SE criteria). (**B**) The LASSO coefficient profiles of the 9 features. The coefficient profile plot was evaluated against the log (lambda) sequence. Vertical line was shown at the value selected using cross-validation, where the optimum lambda gave rise to four features with nonzero coefficients.

Figure 3. The results of the logistic regression analysis among API, FIB-4, FibroQ, and King's score that selected by the LASSO regression model were presented in forest plot.
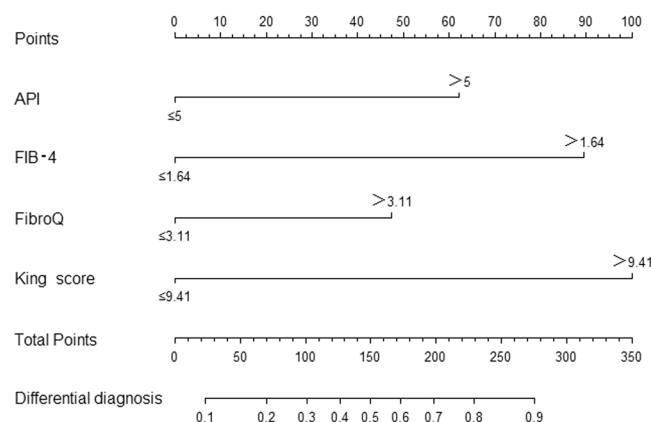
Figure 4. Developed differential diagnosis nomogram for distinguishing HAE and liver cancer. To utilize the nomogram, an individual patient's value was presented on each variable axis, and a vertical line was drown upward to find the number of points received for each variable value. The sum of the variable values was presented on the total point axis, and a vertical line was also drawn downward to the differential diagnosis axes to seek the probability of liver cancer.

examination after surgical resection or preoperative fine needle aspiration biopsy. Therefore, a novel, non-invasive method is required to distinguish HAE from liver cancer before performing all kinds of therapies.

Platelet plays a crucial role in angiogenesis, shortening the time of wound healing, promoting liver regeneration, etc[17]. But, this is just one aspect of the PLT mechanism. When a tumor forms, tumor cells can disrupt the balance of the coagulation system by producing higher levels of coagulation factors. At the same time, the disorders of the coagulation system could also activate more levels of PLTs[18,19]. The activated PLTs provided the procoagulant surface to raise tumor-related gather. Tumor cells were surrounded by activated PLTs and then were escaped from the body's immune detection, which promoted the growth and metastasis of the tumor. However, there is no such series of changes in the blood system and coagulation system during HAE formation. The PLT-based score models that based on blood system, coagulation system, and other factors is constructed in previous reports. But, they emphasized only the significance of recurrence and prognosis that associated with PLT-based score models. Therefore, we want to illustrate that the PLT-based score models are important factors for distinguishing HAE from liver cancer in our study.

To eliminate HBV interference and make the study more convincing, we include all patients with positive of HBsAg, HBeAg or HBeAb, and HBcAb. This model is widely applicable to patients with hepatitis B and non-hepatitis B. Since some factors could also cause fibrosis in HAE patients (not all liver cancer patients existed fibrosis), our study did not determine HAE or liver cancer solely based on the presence or absence of fibrosis. We use the level of fibrosis to comprehensively determine whether the patient is HAE or liver cancer. If a HAE patient with cirrhosis didn't have a corresponding level of PLT-based score, there is a high probability that he or she is not liver cancer (the degree of fibrosis was not enough). Similarly, a liver cancer without cirrhosis (non-cirrhotic HCCs) had a high level of PLT-based score, there is a high probability that he or she is liver cancer.

Previous studies had only found that the possible risk factors were associated with the prognosis and diagnosis of disease, but it was not clear to what extent the factors were associated with the disease status. The nomogram is widely used as a predictive model in tumor and non-tumor diseases, and it could accurately predict disease status based on the degree of correlation between factors and disease[20]. Furthermore nomogram also provides tailored assessments of risk for specific patients and stratifies patients or patient groups by establishing risk thresholds for treatment decisions. That is something that other models don't have.

We develops and validates a diagnostic, PLT-based score models nomogram for the preoperative individualized prediction of HAE and liver cancer. The nomogram incorporates four items of the PLT-based score models. Patients are successfully stratified by the histopathological results. Incorporating the PLT-based score models and PLT count into a user-friendly nomogram verifies the preoperative individualized predictive value of HAE and liver cancer. For developing the nomogram, 9 PLT-based score models factors are reduced to 4 possible indicators by LASSO analysis method that was used to reduce the regression coefficient to examine the correlation of the predicted results. Furthermore, 4 PLT-based score models selected by LASSO regression model are also evaluated by the binomial logistic regression analysis, and results show King's score has an optimum diagnostic value compared with the other three factors. King's score could independently predict HAE and liver cancer (p = 0.0388). But, we still choose to include three other factors because the AUC shows that API, FIB-4 and FibroQ also have a good diagnostic value. Furthermore, the AUC results also show that combining King's score with three other factors (API, FIB-4 and FibroQ) in diagnosing HAE and liver cancer is of better value.

In recent studies, multi-biomarker analysis that incorporates a solitary biomarker into biomarker panels has been widely used[21,22]. For example, a 21-gene test identified and validates the avoidance of chemotherapy in patient with breast cancer[23]. Similarly, the predictive nomogram that incorporates PLT-based score models demonstrates a good discrimination in our research (C-index, 0.929). Furthermore, our simplified nomogram also showed a good identification capability in the validation group (C-index, 0.919). It is reported that the
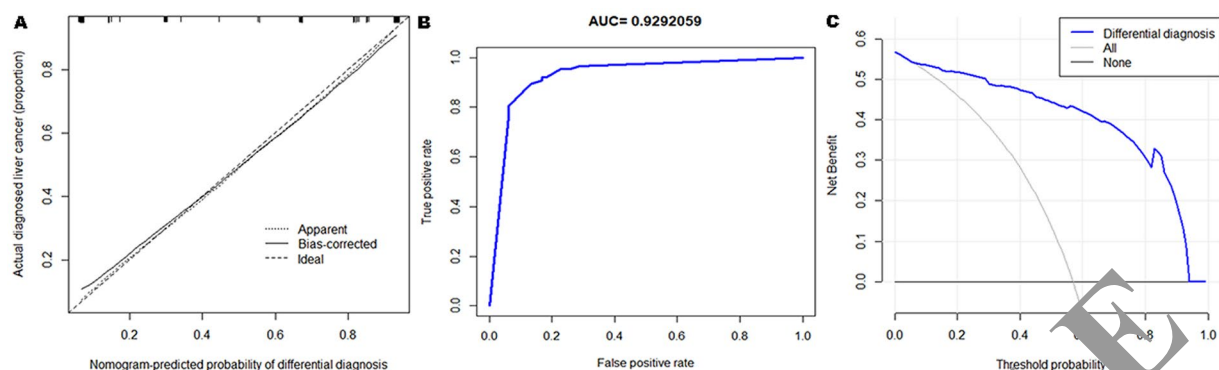
Figure 5. (**A**) The calibration curves of differential diagnosis nomogram prediction in the cohort. The x-axis showed the predicted liver cancer. The y-axis showed the actual diagnosis. The solid line indicated the performance of the nomogram, of which an almost close to the diagonal dotted line presented a good predicted capability. (**B**) The ROC curve for the simplified differential diagnosis nomogram to verify the predicted capability of the model. (**C**) The decision curve analysis for the simplified nomogram. The y-axis measures the net benefit. The blue line showed the differential diagnosis nomogram. The thin solid line presented the assumption that all patients were distinguished. The thin thick solid line showed the assumption that no patients were distinguished. The decision curve showed that if the threshold probability of a patient or doctor is >6%, using the nomogram to diagnose HAE or liver cancer could acquire much more benefit. Within this range, net benefit was comparable, with several overlaps, on the basis of the differential diagnosis nomogram.

accuracy of diagnosis on preoperative peripheral blood tumor marker, such as carcinoembryonic antigen (CEA) and peripheral inflammatory factors, for lymph node metastasis of colorectal cancer was less than 70%, much lower than the C-index of PLT-based score models we constructed[24]. Therefore, the noninvasive, simplified prediction nomogram that incorporated the routine laboratory tests we already get for available, which could regard as a more simplified model for distinguishing HAE from liver cancer.

Both doctors and patients could also perform an individualized diagnosis model for predicting the probability of HAE and liver cancer with the easy feasible scoring system, which is in line with the current concept of precision medicine[25]. However, the clinical outcomes, the particular level of identification or degree of calibration, could not be got by the prediction capability, identification capability and calibration of nomogram[26,27]. The decision curve of our nomogram presented that if the threshold probability of an individual is more than 6%, using the differential diagnosis nomogram in our current research to distinguish HAE from liver cancer would get much more advantage than either distinguishing-all-patients or distinguishing-none.

Conclusion

This research presents a differential diagnosis nomogram that incorporates the PLT-based score models, which could be easily performed to promote the pre-therapy individualized diagnosis of HAE and liver cancer.

Methods

This study was approved by the Institutional Research Ethics Board of Affiliated Hospital of Qinghai University, and all methods were performed in accordance with the Declaration of Helsinki (P-SL-2018005). All patients signed the written informed consent before surgery. This study did not involve human or animal tissue or blood samples.

Patients. We retrospectively collected the demographic, clinical characteristics, and peripheral blood data of 153 patients in the Department of Hepatopancreatobiliary Surgery at the Affiliated Hospital of Qinghai University (Qinghai, China) and the Department of General Surgery at the Shanghai Fourth People's Hospital (Shanghai, China) between November 2011 and December 2018. The 153 patients was divided into two groups: (i) HAE group (66) recruited from the Affiliated Hospital of Qinghai University and (ii) liver cancer group (87) recruited from the two hospitals. All peripheral blood parameters are derived from blood draws taken within 7 days before all kinds of therapies. All patients, including HAE and liver cancer, have been confirmed by surgery or ultrasound guided fine needle aspiration biopsy. Atypical liver cancer is defined that 2 doctors (at least the associate chief physician) are unable to definitively diagnose liver cancer or HAE according to imaging characteristics and peripheral blood tumor markers before surgery. The CT features of atypical liver cancer are cystic lesion, no pseudocapsule, no dynamic scanning enhancement, and no portal vein invasion or tumor thrombus formation. Patients who have one of the following would be excluded: (i) combined with imaging characteristics and peripheral blood tumor markers, the diagnosis could be confirmed; (ii) patients with hematological system diseases; (iii) patients have received the blood transfusion within the previous 6 months; (iv) patients with incomplete clinical data; (v) patients comorbid with non-alcoholic steatohepatitis (NASH), long-term alcohol, long-term oral drugs, etc. The coding system is performed to assure the anonymity of all patients enrolled into the study.

Platelet-based score models. Electronic medical records are used to obtain relevant information, including age, sex, levels of alanine aminotransferase (ALT), aspartate aminotransferase (AST), PLT, international

Index	Formulas
Pohl score	1: AAR > 1 and PLT < 150 × 10⁹/L or else, the score = 0
AARP	1: AAR > 1 or PLT < 150 × 10⁹/L or else, the score = 0
API	Age (years): < 30 = 0; 30–39 = 1; 40–49 = 2; 50–59 = 3; 60–69 = 4; ≥ 70 = 5. PLT: ≥ 225 = 0; 200–224 = 1; 175–199 = 2; 150–174 = 3; 125–149 = 4; < 125 = 5 API is the sum of age and platelet scores and therefore varied from 0–10
CDS	PLT: > 340 = 0; 280–339 = 1; 220–279 = 2; 160–219 = 3; 100–159 = 4; 40–99 = 5; < 40 = 6 ALT/AST ratio: > 1.7 = 0; 1.2–1.7 = 1; 0.6–1.19 = 2; < 0.6 = 3 INR: < 1.1 = 0; 1.1–1.4 = 1; > 1.4 = 2 CDS is the sum of the above
FIB-4	[age (years) × AST (U/L)] / [PLT(109/L) × ALT(U/L)$^{1/2}$]
FibroQ	10 × (Age × AST × PT INR/ALT × PLT)
GUCI	AST × INR × 100/PLT (10⁹/L)
King's score	Age × AST × INR/PLT(10⁹/L)

Table 2. Scoring of platelet-based models. Abbreviation: PLT, Platelet count; AAR, Aspartate aminotransferase/alanine aminotransferase ratio; AARP, AAR-platelet count score; API, age/ platelet count index; CDS, Cirrhosis discriminant score; FIB-4, Fibrosis index based on the four factors; FibroQ, Fibro-quotient; GUCI, Goteburg University Cirrhosis Index; King's score, Fibrosis index based on the four factors; ALT, Alanineaminotransferase; AST, Aspartateaminotransferase; PT, Prothrombin time; INR, internationalnormalized ratio.

normalized ratio (INR), prothrombin time (PT), etiology (hepatitis B virus, HBV), and so on. The Pohl score[28], AARP,[29] API[30], CDS[31], FIB-4[32], FibroQ[12], GUCI[33], and King's score[11] are constructed as described in Table 2.

Statistical analysis. Statistical analysis of the numerical variables among the two groups is performed using unpaired Student's t-test for parametric data or Mann-Whitney rank sum test for nonparametric data. P-value < 0.05 is considered that the difference is statistically significant. The specificity and sensitivity are evaluated by the numerical integration of ROC. And the optimum cut-off point of each variable, the sum of specificity and sensitivity is the highest cumulative value, is obtained by the ROC. Figures are plotted by the GraphPad Prism 5.01 (https://www.graphpad.com/). A bilateral P value < 0.05 is considered statistically significant. All above analyses are performed using SPSS 23.0 software (IBM Corporation, 2015, USA).

The LASSO, particularly suits to the reduction in high dimensional data, is performed to choose the optimum predictive factors in the differential diagnosis of HAE and liver cancer[34,35]. Factors with nonzero coefficients in the LASSO regression model should be chosen. Multivariate analysis is performed to construct a predicting model by combining the factors selected in the LASSO regression model. The result is presented in a figure using the stata15.0 (https://www.stata.com). Figure is characterized by odds ratio (OR) and 95%CI. Variables chose by LASSO regression model are included in the model. All possible diagnostic factors are performed to construct a simplified model for the differential diagnosis of HAE and liver cancer[25,37]. A simplified nomogram is showed based on the result of LASSO regression model. The Harrell's concordance index (C-index) is performed to quantify the discrimination performance of the simplified nomogram. In general, the value of C-index greater than 0.75 is regarded as a relatively good discrimination[38]. The calibration curves are plotted to evaluate the predictive ability of the nomogram related with platelet-based models[39]. The bootstrapping method is performed to reduce estimate bias. The predictive nomogram of platelet-based models is conducted to bootstrapping validation (10000 bootstrap resamples) to count a relatively corrected C-index[40]. The decision curve is presented to evaluate the net benefits of different threshold probabilities for individuals to confirm clinical usefulness of the simplified nomogram[41]. The net benefit is counted by subtracting the proportion of all patients who are false positive from the proportion of the patients who are true positive and by weighing the relative harm of forgoing interventions compared with the negative consequences of an unnecessary intervention[42]. In this study, discrimination is also evaluated using the AUC of ROC. An AUC of a diagnostic nomogram less than 0.5 states no predictive advantage over an assumed 50% probability of either outcome, whereas a value of 1.0 states wonderful predictive capacity of the nomogram. All of these statistical methods are performed by R software version 3.6.0 (http://www.rproject.org) with R packages "rms", "glmnet", "Hmisc", "ROCR", "rmda", "caret", and "foreign".

Data availability
The datasets generated during and/or analyzed during the current study are available from the corresponding author on reasonable request.

References
1. Carmena, D. & Cardona, G. A. Echinococcosis in wild carnivorous species: epidemiology, genotypic diversity, and implications for veterinary public health. *Vet Parasitol* **202**, 69–94 (2014).
2. Farrokh, D., Zandi, B., Pezeshki Rad, M. & Tavakoli, M. Hepatic Alveolar Echinococcosis. *Arch Iran Med* **18**, 199–202 (2015).
3. Lötsch, F. *et al.* FDG-PET/MRI imaging for the management of alveolar echinococcosis: initial clinical experience at a reference centre in Austria. *Trop Med Int Health* **24**, 663–670 (2019).
4. Filippou, D., Tselepis, D., Filippou, G. & Papadopoulos, V. Advances in liver echinococcosis: diagnosis and treatment. *Clin Gastroenterol Hepatol* **5**, 152–159 (2007).
5. Du, Q. C., Zhou, Y. & Fan, H. N. Treatment of hepatic alveolar echinococcosis infringing the inferior vena cava. *Rev Soc Bras Med Trop* **52**, e20180342 (2019).

6. Serper, M. *et al*. Association of Provider Specialty and Multidisciplinary Care With Hepatocellular Carcinoma Treatment and Mortality. *Gastroenterology* **152**, 1954–1964 (2017).
7. El-Serag, H. B. Hepatocellular Carcinoma. *N Engl J Med* **365**, 1118–1127 (2011).
8. Du, Q. C. *et al*. A new treatment strategy for end-stage hepatic alveolar echinococcosis: IVC resection without reconstruction. *Sci Rep* **9**, 9419 (2019).
9. Sulima, M. *et al*. Liver Transplantation for Incurable Alveolar Echinococcosis: An Analysis of Patients Hospitalized in Department of Tropical and Parasitic Diseases in Gdynia. *Transplant Proc* **48**, 1708–1712 (2016).
10. Ozdemir, F. *et al*. Living donor liver transplantation for Echinococcus Alveolaris: single-center experience. *Liver Transpl* **21**, 1091–1095 (2015).
11. Cross, T. J. *et al*. King's Score: an accurate marker of cirrhosis in chronic hepatitis C. *Eur J Gastroenterol Hepatol* **21**, 730–738 (2009).
12. Hsieh, Y. Y. *et al*. FibroQ: an easy and useful noninvasive test for predicting liver fibrosis in patients with chronic viral hepatitis. *Chang Gung Med J* **32**, 614–622 (2009).
13. Toyoda, H., Kumada, T., Tada, T., Kaneoka, Y. & Maeda, A. A laboratory marker, FIB-4 index, as a predictor for long-term outcomes of hepatocellular carcinoma patients after curative hepatic resection. *Surgery* **157**, 699–707 (2015).
14. Lee, Z. & Luo, G. Issues pertaining to PET imaging of liver cancer. *J Fasting Health* **2**, 62–64 (2014).
15. Wang, L., Fan, J., Ding, X., Sun, J. & Zhang, M. Assessment of liver fibrosis in the early stages with perfusion CT. *Int J Clin Exp Med* **8**, 15276–15282 (2015).
16. Sefić Pašić, I. *et al*. Possibilities of differentiation of solitary focal liver lesions by computed tomography perfusion. *Med Glas (Zenica)* **12**, 144–150 (2015).
17. Kondo, R., Nakashima, O., Tanikawa, K., Nomura, Y. & Kage, M. Accumulation of platelets in the liver may be an important contributory factor to thrombocytopenia and liver fibrosis in chronic hepatitis C. *J Gastroenterol* **48**, 526–534 (2013).
18. Myriam, L., Shahinoor, B. & Hynes, R. O. Direct signaling between platelets and cancer cells induces an epithelial-mesenchymal-like transition and promotes metastasis. *Cancer Cell* **20**, 576–590 (2011).
19. Bambace, N. M. & Holmes, C. E. The platelet contribution to cancer progression. *J Thromb Haemost* **9**, 237–249 (2011).
20. Xu, X. P. *et al*. A predictive nomogram for individualized recurrence stratification of bladder cancer using multiparametric MRI and clinical risk factors. *J Magn Reson Imaging* (2019). https://doi.org/10.1002/jmri.26749
21. Roberta, V. & Claudia, P. Roberta, C. & Ciro, I. Patented Biomarkers for the Early Detection of Ovarian. *Cancer. Recent Pat Biomark* **100**, 1–9 (2011).
22. Zhao, S. *et al*. Three inflammation-related genes could predict risk in prognosis and metastasis of patients with breast cancer. *Cancer Med* **8**, 593–605 (2019).
23. Sparano, J. A. *et al*. Prospective Validation of a 21-Gene Expression Assay in Breast Cancer. *N Engl J Med* **373**, 2005–2014 (2015).
24. Toiyama, Y. *et al*. Serum Angiopoietin-like Protein 2 Improves Preoperative Detection of Lymph Node Metastasis in Colorectal Cancer. *Anticancer Research* **35**, 2849–2856 (2015).
25. Balachandran, V. P., Gonen, M., Smith, J. J. & DeMatteo, R. P. Nomograms in oncology: more than meets the eye. *Lancet Oncol* **16**, e173–e180 (2015).
26. Localio, A. R. & Goodman, S. Beyond the usual prediction accuracy metrics: reporting results for clinical decision making. *Ann Intern Med* **157**, 294–295 (2009).
27. Van Calster, B. & Vickers, A. J. Calibration of risk prediction models: impact on decision-analytic performance. *Med Decis Making* **35**, 162–169 (2015).
28. Shahid, M. *et al*. Correlation of biochemical markers and HCV RNA titers with fibrosis stages and grades in chronic HCV-3a patients. *Eur J Gastroenterol Hepatol* **26**, 788–794 (2014).
29. Lee, I. C. Comparative analysis of noninvasive models to predict early liver fibrosis in hepatitis B e Antigen-negative Chronic Hepatitis B. *J Clin Gastroenterol* **45**, 278–285 (2011).
30. Poynard, T. & Bedossa, P. Age and platelet count: a simple index for predicting the presence of histological lesions in patients with antibodies to hepatitis C virus. METAVIR and CLINIVIR Cooperative Study Groups. *J Viral Hepat* **4**, 199–208 (2010).
31. Li, Q., Lu, C., Li, W., Huang, Y. & Chen, L. Evaluation of eLIFT for Non-invasive Assessment of Liver fibrosis and Cirrhosis in Patients with Chronic Hepatitis B Virus Infection. *Sci Rep* **7**, 5429 (2017).
32. Sterling, R. K. *et al*. Development of a simple noninvasive index to predict significant fibrosis in patients with HIV/HCV coinfection. *Hepatology* **43**, 1317–1325 (2010).
33. Islam, S. Cirrhosis in hepatitis C virus-infected patients can be excluded using an index of standard biochemical serum markers. *Scand J Gastroenterol* **40**, 867–872 (2005).
34. Sauerbrei, W., Royston, P. & Binder, H. Selection of important variables and determination of functional form for continuous predictors in multivariable model building. *Stat Med* **26**, 5512–5528 (2007).
35. Friedman, J., Hastie, T. & Tibshirani, R. Regularization paths for generalized linear models via coordinate descent. *J Stat Softw* **33**, 1–22 (2016).
36. Kidd, A. *et al*. Survival prediction in mesothelioma using a scalable Lasso regression model: instructions for use and initial performance using clinical predictors. *BMJ Open Respir Res* **5**, e000240 (2018).
37. Iasonos, A., Schrag, D., Raj, G. V. & Panageas, K. S. How to build and interpret a nomogram for cancer prognosis. *J Clin Oncol* **26**, 1364–1370 (2008).
38. Han, D. S. *et al*. Nomogram Predicting Long-Term Survival After D2 Gastrectomy for Gastric Cancer. *J Clin Oncol* **30**, 3834–3840 (2012).
39. Kramer, A. A. & Zimmerman, J. E. Assessing the calibration of mortality benchmarks in critical care: The Hosmer-Lemeshow test revisited. *Crit Care Med* **35**, 2052–2056 (2007).
40. Nie, R. *et al*. Risk-stratification model to select conversion surgery for advanced gastric cancer patients. *Chin J Cancer Res* **31**, 178–187 (2019).
41. Vickers, A. J., Cronin, A. M., Elkin, E. B. & Gonen, M. Extensions to decision curve analysis, a novel method for evaluating diagnostic tests, prediction models and molecular markers. *BMC Med Inform Decis Mak* **8**, 53 (2008).
42. Huang, Y. Q. *et al*. Development and validation of a radiomics nomogram for preoperative prediction of lymph node metastasis in colorectal cancer. *J Clin Oncol* **34**, 2157–2164 (2016).

Acknowledgements

Author contributions

Qiancheng Du, Yanyan Wang, Shihao Guan and Chenliang Hu: study design, data collection, analysis, and manuscript writing. Jian Sun and Ying Zhou: manuscript review. Mengxuan Li: data collection and analysis. Ling Zhou, Mengzhao Zhang, Xuepeng Mei and Yichong Chen: data collection.

Competing interests

The authors declare no competing interests.

Additional information

Correspondence and requests for materials should be addressed to J.S. or Y.Z.

Reprints and permissions information is available at www.nature.com/reprints.

Publisher's note Springer Nature remains neutral with regard to jurisdictional claims in published maps and institutional affiliations.